Spatiotemporal pattern in somitogenesis: A non-Turing scenario with wave propagation

Hiroki Nagahara,[1,*] Yue Ma,[2,†] Yoshiko Takenaka,[3,‡] Ryoichiro Kageyama,[4,5,§] and Kenichi Yoshikawa[1,2,‖]

[1]*Department of Physics, Graduate School of Science, Kyoto University, Kyoto 606-8502, Japan*

[2]*Spatio-Temporal Order Project, ICORP, Japan Science and Technology Agency (JST), Tokyo 102-0075, Japan*

[3]*Venture Business Laboratory, Kyoto University, Kyoto 606-8501, Japan*

[4]*Institute for Virus Research, Kyoto University, Kyoto 606-8507, Japan*

[5]*CREST, Japan Science and Technology Agency, Kyoto 606-8507, Japan*

(Received 6 March 2009; published 11 August 2009)

Living organisms maintain their lives under far-from-equilibrium conditions by creating a rich variety of spatiotemporal structures in a self-organized manner, such as temporal rhythms, switching phenomena, and development of the body. In this paper, we focus on the dynamical process of morphogens in somitogenesis in mice where propagation of the gene expression level plays an essential role in creating the spatially periodic patterns of the vertebral columns. We present a simple discrete reaction-diffusion model which includes neighboring interaction through an activator, but not diffusion of an inhibitor. We can produce stationary periodic patterns by introducing the effect of spatial discreteness to the field. Based on the present model, we discuss the underlying physical principles that are independent of the details of biomolecular reactions. We also discuss the framework of spatial discreteness based on the reaction-diffusion model in relation to a cellular array, by comparison with an actual experimental observation.

DOI: 10.1103/PhysRevE.80.021906 PACS number(s): 87.18.Hf, 82.40.Ck, 47.54.Fj

I. INTRODUCTION

Living organisms maintain their existence through the generation of temporal rhythms, switching phenomena, and spatiotemporal structures that appear in a self-organizing manner under far-from-equilibrium conditions. In particular, the developmental processes of higher animals, where each individual organism creates complex structures from a spherical egg accompanied by symmetry breaking, have fascinated many scientists, including mathematicians and physicists, as well as biologists.

Ever since Turing proposed the epoch-making idea that morphogens can self-organize into stationary patterns based on the neighboring interactions among local kinetics, i.e., reaction and diffusion [1], extensive studies have revealed that nonlinear reaction-diffusion systems are quite effective for interpreting many real spatiotemporal patterns in biological systems [2,3], where the best-known example may be the coat patterns of animals and fish [4,5]. Other applications of reaction-diffusion systems in biological systems include the spatiotemporal behavior in the fusion and partial separation of plasmodia of a slime mold [6–8], excitable pulses in nervous systems [3], and the rhythmicity of cardiac tissues [9].

Despite previous successes, there is increasing criticism regarding the application of reaction-diffusion models with a Turing structure to real biological systems. An important issue is that, to create a stationary spatiotemporal pattern with a reaction-diffusion model, the local kinetic units must show two different types of interaction between neighboring cells: the diffusion of an activator and a much greater diffusion (long-range diffusion) of an inhibitor. However, this raises the question of whether long-range diffusion of the inhibitor is universal in biological systems. Moreover, the Turing structure has been considered with regard to spatially continuous media. Although spatial continuity is acceptable in most chemical reaction systems, this is usually not the case in biological systems, simply because the cells in a multicellular organism have a finite size. In some situations, the scale of the spatiotemporal pattern of interest is much larger than that of individual cells, and hence, the mathematical model can support this assumption of a continuum. However, if we consider the initial stage of the developmental process, when many important biological patterns emerge, the number of cells is usually small and their size cannot be neglected since the field size where the phenomena occur is comparable to that of a cell. In addition, since diffusion inside a cell is quite fast compared to both diffusion across a membrane and the time scale of cell dynamics [10], instead of considering spatial variation within single cells, cells can be regarded as interacting discrete nodes in a network. More importantly, from a mathematical perspective, it has been suggested that the discreteness of reaction-diffusion systems can lead to spatiotemporal patterns in another way, which is impossible for the case of a continuum [11].

In this paper, we focus on the dynamic process of morphogenesis in somitogenesis. It has been observed that the propagation of gene expression inspired by a segmentation clock produces spatially periodic patterns in the vertebral column. Somites are transient units that form repetitive body structures such as vertebrae, ribs, and skeletal muscles. In mice and snakes, they are generated regularly by a segmentation process of the presomitic mesoderm (PSM) from the anterior-most end [12–14]. Most recently, a similar dynamic gene expression has also been confirmed in spider [15].

*Present address: Mitsubishi UFJ Securities Co., Ltd., Tokyo 100-6317, Japan; nagahara-hiroki@sc.mufg.jp

†Corresponding author; dr.mayue@gmail.com

‡Present address: RIKEN Advanced Science Institute, Saitama 351-0198, Japan; ytakenaka@riken.jp

§rkageyam@virus.kyoto-u.ac.jp

‖yoshikaw@scphys.kyoto-u.ac.jp

 ©2009 The American Physical Society

Based on experimental observations, it has been revealed that, during somitogenesis, the expression level of some genes sweeps across a field of cells, as in wave propagation [16,17]. These genes express periodically at the posterior end of the PSM, where a so-called "segmentation clock" works [12,13,7,18,19]. As it propagates to the anterior end of the PSM, the wave gradually slows down, shrinks in width, and finally stops as an additional stationary band at the determination front, where a new segment is generated [12,13,16]. In the case of a mouse embryo, the PSM is only about 50 cells (total length of the PSM is about 500 μm whereas the diameter of a single cell is about 10 μm). Thus, it is crucially important to take the natural characteristics of the spatial discreteness of the system into consideration.

To understand how clock oscillation is generated and how it regulates segmentation, many attempts have been made to create mathematical models. A simple ordinary differential equation model was first proposed by Goodwin based on a negative-feedback process in gene expression [20,21]. Recently, more sophisticated models have been proposed to explain oscillatory gene expression by taking into account a time delay [22], a positive-feedback loop [23], or some environmental factors [24]. Some models have also been proposed to determine the spatial information of segmentation. The most well-known model is probably the "clock and wavefront" model, which was originally proposed by Cooke and Zeeman [25]. It introduced the interaction between a positional information gradient with biological oscillation. However, this idea remained just a theoretical concept until it recently gained experimental support [19,26,27]. Since then, many mathematical attempts have been made to reproduce a clock and wave front scenario [28–33]. There are also many other frameworks, such as the reaction-diffusion model [34], clock and trail model [35], cellular oscillator model [36], and so on.

Despite the success in the application of a mathematical approach to somitogenesis, there are still many limitations. First, many models control the specific position of spatial strips "manually," by defining thresholds or piecewise functions. This is in contrast to the principal of the self-organization of biological systems. Second, models based on a continuum suffer from the difficulty of producing a narrow boundary between two phenotypes [37,38] as sharp as two to three cells. Finally, most current models assume the existence of two or more different types of interactions among the neighboring cells, which are often introduced as diffusions of an activator and inhibitor, which represent positive and negative interactions, respectively.

In this paper, we present a simple one-dimensional reaction-diffusion model that includes two hypothetical substances. There are three features in our model: (1) no inhibitory interaction, (2) cell discreteness, and (3) spatial inhomogeneity. We will demonstrate how a spatially periodical pattern with sharp boundaries from a smooth signal gradient can be generated with a combination of cellular oscillation and wave propagation. Although the proposed model is highly abstract and idealized in the context of biology, we keep in mind that the underlying physical aspects are beyond the details of biochemical processes; they are more general and independent of species. Based on our simple model, we will introduce two kinds of length scales, which are reasonable for the interaction length among neighboring cells, and for judging whether discreteness will affect the dynamics.

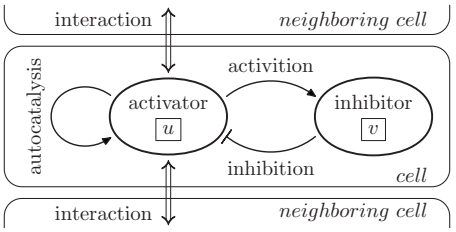

FIG. 1. Illustration of a reaction-diffusion system (activator-inhibitor type). Note that we exclude the diffusion of the inhibitor v, i.e., Turing instability can never be satisfied in our model.

II. DESCRIPTION OF THE MODEL

As a hypothetical model that describes the above characteristics of gene expression in somitogenesis, we introduce a set of discrete reaction-diffusion equations

$$\frac{\partial u}{\partial t} = f(u,v) + D\mathcal{L}u,$$

$$\frac{\partial v}{\partial t} = g(u,v), \tag{1}$$

where u and v are the intracellular concentrations of the activator and inhibitor, respectively. The reaction terms of the activator and inhibitor are given as follows:

$$f(u,v) = \frac{1}{\tau_1}\left(\frac{1}{\gamma}u(u-\alpha)(1-u) - v + \beta\right),$$

$$g(u,v) = \frac{1}{\tau_2}(u-v), \tag{2}$$

where τ_1 and τ_2 present the characteristic time scales of the local reaction kinetics of u and v, respectively. The parameter γ depends on space x and/or time t to represent the spatial gradient and the temporal change in the concentration of a certain substance. Its biological counterpart is the morphogen gradient, such as the posterior-anterior concentration gradient of FGF8 protein in PSM, which is considered to play an important role in the formation of periodic patterns in somitogenesis [12,39–41].

Equations (2) are Fitzhugh-Nagumo type of models, which has been well studied for a description of excitable behaviors in biology. We adopt it to study the "activator-inhibitor system" (see e.g., [3]), which includes an autocatalytic property of the activator and a negative-feedback loop of the inhibitor (as shown in Fig. 1). Figure 2 shows the nullclines $f(u,v)=0$ and $g(u,v)=0$. By changing the parameter γ, which adjust the amplitude of cubic function, we can vary the local kinetics from oscillation to bistability [Figs. 2(a) and 2(b)], and avoid happening monostable state.

$\mathcal{L}$ in Eq. (1) is the Laplace operator which is defined as

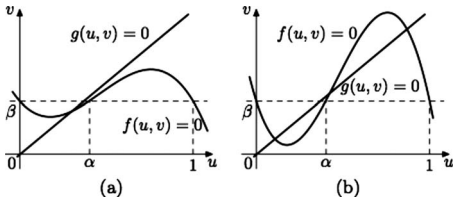

FIG. 2. Geometry of nullclines corresponding to (a) oscillatory state in a big γ case and (b) bistable state when γ is small enough.

$$\mathcal{L}u := \frac{1}{\Delta x^2}\{u(t,x+\Delta x) - 2u(t,x) + u(t,x-\Delta x)\} \tag{3}$$

for a spatially discrete one-dimensional field with a grid size of Δx, or

$$\mathcal{L}u := \frac{\partial^2 u(t,x)}{\partial x^2} \tag{4}$$

for a spatially continuous field (i.e., in the limit $\Delta x \to 0$). Although cell to cell interaction may take place in many different ways, such as membrane protein signaling, we adopt a diffusionlike coupling between activator u in this paper without losing generality. D indicates the strength of interaction among neighboring cells. We need to emphasize that the model in Eq. (1) does not include the diffusion term of the inhibitor v, and, hence, it never shows Turing instability.

III. SIMULATION RESULTS

Numerical simulations are carried out on a one-dimensional field by substituting Eqs. (2) and (3) into Eq. (1). The spatial and temporal units are normalized as 1 mm and 1 min, respectively. Based on the actual cell size (about 10 to 15 μm), we choose the spatial mesh size as $\Delta x = 0.01$. Numerical simulations are performed with the following constant parameters:

$$\tau_1 = 0.588, \quad \tau_2 = 32.1, \quad D = 1.19 \times 10^{-5},$$

$$\alpha = 0.40 \text{ and } \beta = 0.33. \tag{5}$$

These values are chosen based on the details that we will discuss later in Sec. IV.

Figure 3 shows the results of the numerical simulations in spatiotemporal diagrams. Figure 4 illustrates the manner of wave propagation and the variation in γ in one-dimensional reaction-diffusion fields.

A. Gradation of γ leads to a standing pulse

Usually, the profile of γ can be determined by diffusion and degradation. For the sake of simplicity, we choose it as a linear gradient function.

$$\gamma(x) = 0.21 - 0.20x, \quad x \in [0,1]. \tag{6}$$

Since we discuss the phenomena in a normalized field, we do not consider its relevance to spatial dependence, which is usually important in development biology. In Fig. 3(a), a pulse is triggered at the left boundary ($x=0$) and propagates to the right. It shrinks in width, and finally stands at a certain point, due to the decrease in γ [see Fig. 4(a)]. The standing pulse is stable and does not vanish after it stops. Here, the wave front and back have different critical values of γ, below which they cannot propagate any further.

B. Generation of spatially periodic pattern

Next, we consider dynamical cases where γ changes temporally, and produce spatially periodic stationary patterns. We consider two cases: the growth of an embryo and an antagonist of a morphogen [42].

If we consider the growth of an embryo, the parameter γ depends not only on spatial distribution, but also on temporal evolution. We assume that it satisfies the following equations:

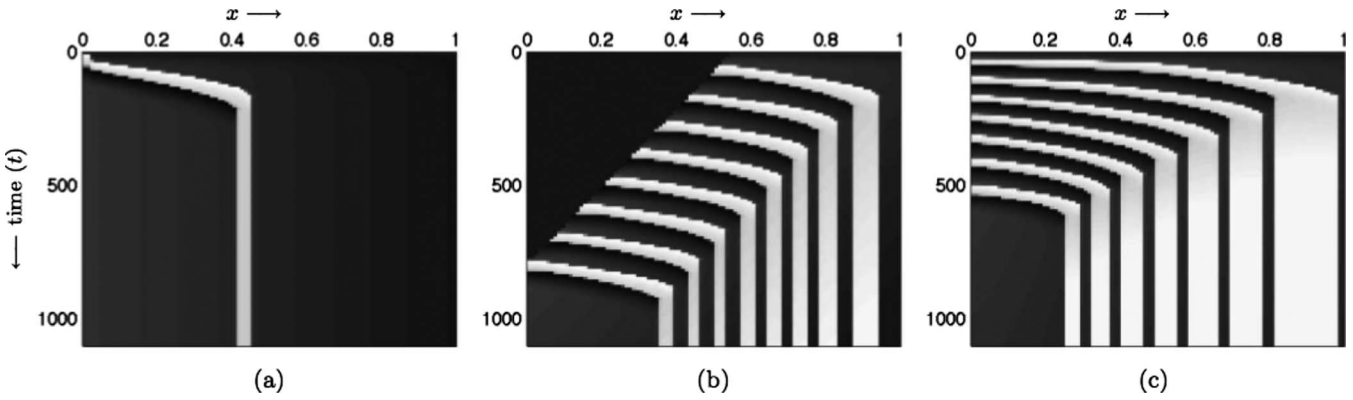

FIG. 3. Spatiotemporal diagrams of $u(t,x)$ illustrating the manner of wave propagation, depending on the geometrical distribution of γ. The grayscale from black to white indicates the level of u from 0 to 1. (a) Parameter γ is given as an invariant spatial gradient. A single pulse triggered at the left boundary propagates to the right, and finally generates a stationary band at a specific position. (b) If we consider the growth of the embryo (the posterior end of PSM grows from $x=0.55$ to $x=1$), the kinetic parameter γ is a function of both space and time. In this case, a pulse train leads to a static, periodic structure. (c) Parameter γ is set to decrease as a wave passes, while we ignore the growth of the embryo. The pulse train can also cause a static periodic structure. In contrast to (b), there is large diversity in the band width of the final pattern.

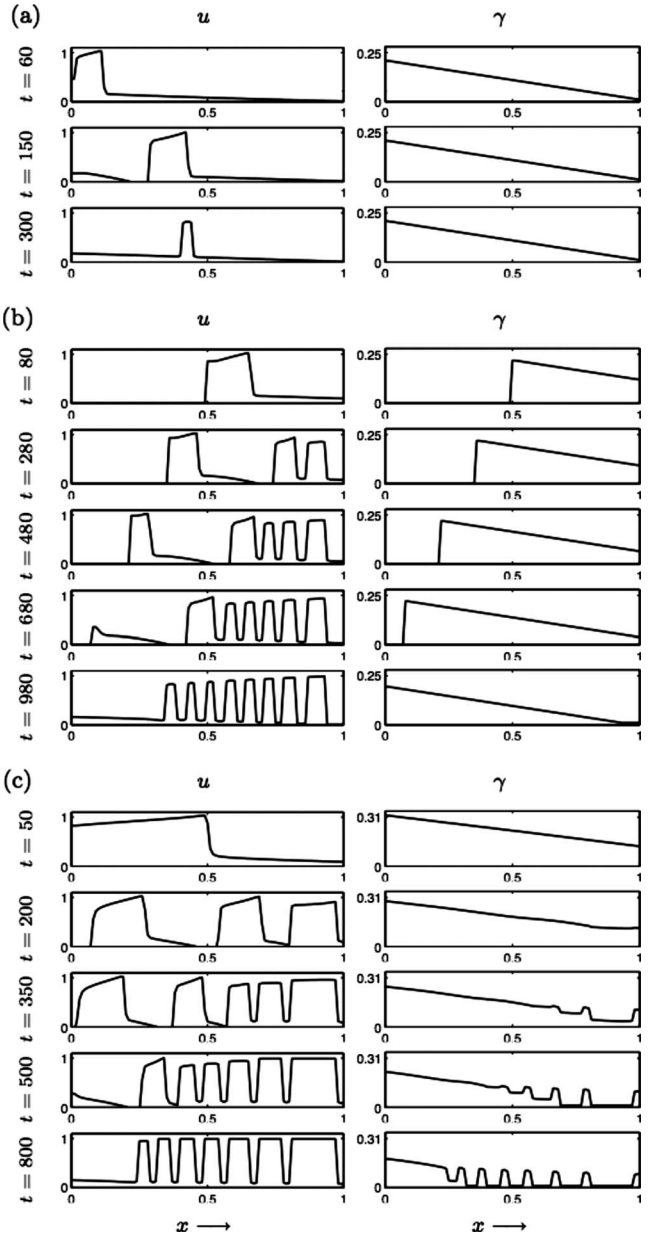

FIG. 4. Snapshots at different time points. Left and right columns show the time evolutions of u and γ, respectively. (a), (b), and (c) correspond to three cases as shown in Fig. 3.

$$\gamma(t,x) = \tilde{\gamma}(t - t_x) = 0.22 - 1.38 \times 10^{-4}(t - t_x),$$

$$t_x = 1.45 \times 10^3(0.55 - x), \tag{7}$$

where t_x denotes the birth time of the cell at position x. The state variables $u(t,x)$ and $v(t,x)$ are taken to be zero before the birth of the cell, i.e., $t < t_x$. Thus, we have a critical line, $t = 1.45 \times 10^3(0.55 - x)$, in the spatiotemporal plot [Fig. 3(b)], above which no cell exists. This line corresponds to the position of the posterior end of the growing PSM. As shown in the right column in Fig. 4(b), the gradient of γ has its highest concentration at the posterior end, which is moving leftward as defined by $x = 0.55 - 6.9 \times 10^{-4}t$. Correspondingly, the length of PSM grows from 0.45 to 1. On the other hand, the left column in Fig. 4(b) shows a series of pulses that are periodically triggered by a biological clock at the left (posterior) moving end. The pulse train propagates to the right (anterior side) and forms a stationary and spatially periodic structure. The output pattern fits the observation in [27].

In the last stage of somitogenesis, several somites are still generated when the growth of PSM slows down or even stops [43]. Regarding these cases, we consider the situation that γ is locally inhibited by v, and seize the growth of the embryo. The parameter γ is governed by

$$\frac{\partial \gamma(t,x)}{\partial t} = -6.0 \times 10^{-4} v\, \theta(\gamma - 0.01),$$

$$\text{initial condition: } \gamma(0,x) = 0.33 - 0.20x, \tag{8}$$

where $\theta(\gamma - 0.01)$ is the Heaviside step function, which prevents γ from being less than 0.01. The simulation results are shown in Figs. 3(c) and 4(c). A series of pulses are triggered from the oscillatory region at the left fixed end and propagate to the right. At the same time, the concentration of γ decreases globally, corresponding to the distribution of the inhibitor v. This model shows that a spatial periodic structure in the bistable region can be autonomously generated even without the aid of embryo growth.

IV. DISCUSSION

Based on our numerical simulations, we can conclude that the interesting characteristics of gene expression in somitogenesis can be reproduced by a simple discrete reaction-diffusion system. The generated pattern is robust because the interface is pinned in the bistable region of the cell chain. To make cells transit from one state to the other, it needs to overcome a high energy barrier, which is usually difficult in a weak-coupling situation. Based on the present simple model, we can infer some important physical aspects of actual somitogenesis, even if the exact biomolecular reactions are still far from being clear.

A. Diffusion length

To judge whether the interaction length between neighboring cells is within a realistic range, it would be useful to define a spatial scale for measurement. This would be an important factor for examining the validity of the proposed model. As a spatial scale, we adopt a diffusion length over which the activator u diffuses during its lifetime.

Let us briefly explain how to estimate the diffusion length by using the relations among the physical quantities in the model of Eqs. (1) and (2). Since the activator u and inhibitor v have quite different time scales $\tau_1 \ll \tau_2$, u reacts much faster than v. Thus, the value of v in the vicinity of the wave front is an approximate constant v^*. Under this condition, the propagation speed c of the traveling waves can be expressed by

$$c = K\sqrt{\frac{D}{\tau_1}}, \tag{9}$$

where K is a dimensionless speed of the wave. For the reaction function of Eq. (2), K can be analytically described by

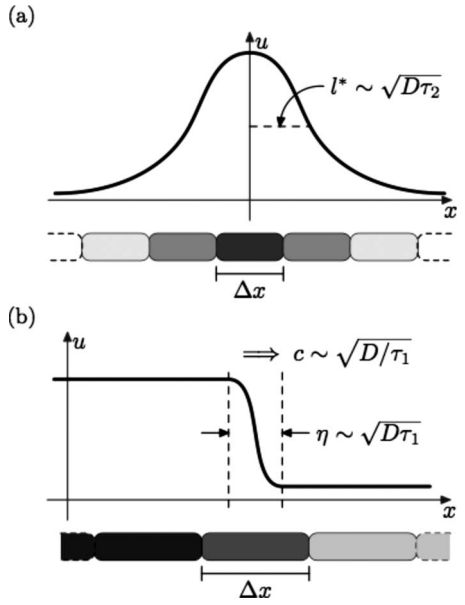

FIG. 5. Two length scales showing the differences between continuous space and a discontinuous cellular array. (a) Characteristic scale l^* represents the diffusion length of activator u in its lifetime. By using the wave velocity c, we can obtain the representation $l^* \sim \sqrt{D\tau_2} = c\sqrt{\tau_1\tau_2}$ which consists of observable quantities. (b) $\eta \sim \sqrt{D\tau_1}$ is the edge width of the traveling wave front in the continuum. By comparing this length scale with the distance Δx between two cells, we can evaluate the discreteness of the field.

$$K = (2\gamma)^{-1/2}\{(u_3^* - u_2^*) - (u_2^* - u_1^*)\} \sim 1, \tag{10}$$

where u_1^*, u_2^*, and u_3^* $(u_1^* \leq u_2^* \leq u_3^*)$ are three roots of $f(u,v^*)=0$. Previous studies have suggested that K is on the order of $\mathcal{O}(1)$ except in some singular situations [44]. Without losing generality, we can simply fix K as unity by ignoring the variation in γ since we are mainly concerned about the physical scale of the model. Moreover, since the large τ_2 implies slow negative feedback on u by v, the lifetime of u can be estimated to be the time scale of v, i.e., τ_2. By using a method similar to that for estimating Kuramoto's length [45,46], we obtain the typical diffusion length of u in its lifetime as

$$l^* \sim \sqrt{D\tau_2} = c\sqrt{\tau_1\tau_2} < c\tau_2, \tag{11}$$

in which effective interaction with a neighboring cell can take place, as illustrated in Fig. 5(a).

A significant feature of the resulting diffusion length is its experimental accessibility. Since parameters c, τ_1, and τ_2 can be measured by appropriate experiments, we can estimate $l^* \sim c\sqrt{\tau_1\tau_2}$ or, at least, the maximum of $c\tau_2$ from experimental data. For example, let us adopt the actual experimental data on somitogenesis in a mouse embryo, where expression of the gene "Hes7" is believed to play an essentially important role (e.g., [16]). Based on experimental observations, the propagation speed of its expression c is about 250 μm/h. Moreover, based on the observation that the half-life of the Hes7 protein is about 22 min [24,47], we obtain that the characteristic time scale of the related reaction is in the order $\tau_2 \approx 22/\ln 2 \approx 30$ min. Thus, by substituting these values into Eq. (11), we obtain $l^* < 13$ μm. This result shows that the diffusion length is less than the scale of a single cell by an order of magnitude (c.f. the diameter of a single cell is usually about 10–15 μm). Thus, it is clear that the reaction-diffusion model proposed in this paper works within a realistic length of interaction among neighboring cells. Furthermore, Eq. (11) does not contain parameters that are specific to some details in the biomolecular reactions. This feature makes it possible to apply the model widely regardless of the great complexity of biomolecular reactions. For example, it would be helpful for identifying the time scale of biomolecular reactions that are related to dynamic gene expressions in biological systems, including somitogenesis.

B. Importance of discreteness

Since our model is based on spatial discreteness, it raises the question of whether discreteness indeed plays a role in multicellular tissue. To answer this question, we introduce another length scale $\eta \sim \sqrt{D\tau_1}$.

As shown in Eq. (9), the propagation velocity of a single pulse is about $c \sim \sqrt{D/\tau_1}$. On the other hand, since the time interval in which the propagating wave front passes a certain point is about τ_1, the length scale of the width of the wave front η is about

$$\eta \sim c \cdot \tau_1 = \sqrt{\frac{D}{\tau_1}}\tau_1 = \sqrt{D\tau_1}, \tag{12}$$

as shown schematically in Fig. 5(b).

Next, for the sake of simplicity, let us consider a reduced one-dimensional reaction-diffusion equation which consists of a bistable medium u,

$$\frac{\partial u(t,x)}{\partial t} = \frac{1}{\tau_1} f(u(t,x)) + D\mathcal{L}u(t,x), \tag{13}$$

$$f(u) = u(u-\alpha)(1-u), \quad \alpha < 1/2. \tag{14}$$

By introducing a dimensionless time $s = t/\tau_1$ and considering spatial discreteness, we get

$$\frac{\boldsymbol{d}u(s,x)}{\boldsymbol{d}s} = f(u(s,x)) + d_c \Delta u, \tag{15}$$

where

$$\Delta u \equiv u(s,x+\Delta x) - 2u(s,x) + u(s,x-\Delta x), \tag{16}$$

$$d_c \equiv \frac{D\tau_1}{(\Delta x)^2}. \tag{17}$$

It has been mathematically proven that, in the bistable medium described by Eqs. (15)–(17), if the coupling strength d_c is small enough, the propagation of a wave front is blocked and there exist inhomogeneous and stable steady solutions [11]. Note that this phenomenon, which is called "wave propagation failure," cannot be observed in the continuous counterpart $(\Delta x \to 0)$. In that case, the wave front will propagate across the field without stopping. Especially, when $f(u)$ is a cubic function as shown in Eq. (14), the criterion is

given as $d_c < \alpha^2/4$ ([11,48]). If we substitute it into Eq. (17), we have

$$\eta \sim \sqrt{D\tau_1} < \frac{\alpha}{2}\Delta x < \frac{1}{4}\Delta x. \tag{18}$$

Consequently, the effect of natural spatial discreteness cannot be negligible when the cell size Δx is larger than $4\sqrt{D\tau_1}$, as an order-of-magnitude estimation. Although this condition tends to be weaker because of the existence of the inhibitor and other parameters of the reaction function, Eq. (18) gives us an intuitive understanding of the importance of discreteness.

Note that in some continuous reaction-diffusion systems, especially those having inhibitor coupling, the stationary state can be obtained by tuning parameters to realize zero velocity. It is a completely different scenario, however, from the mechanism of wave propagation failure in a spatially discrete system. Moreover, in a continuum Turing type of model, the pattern robustness can be obtained by increasing the coupling strength of inhibitor. It is not the case of our model, however, since the inhibitor coupling is absent as Eq. (1) shows. The discrete model ensured its pattern robustness by the weak coupling of activator and the strong bistability, which are small enough, D and γ, correspondingly.

C. Growth rate of the embryo

There is a great variety in somitogenesis in different species. The combination of the growth rate of the embryo and the period of the segmentation clock plays an important role in producing various numbers and sizes of somites. This issue can also be explained by our model.

As introduced in Sec. III B, we adopted the hypothesis that the growth of the embryo determines the distribution of γ through the ages of single cells. We assume that γ is a time-dependent function as indicated in Eq. (7). In the case of the result shown in Fig. 3(b), the birth time t_x of the cell at position x was set as a linear function. Here we go a step further and set t_x as a general function: $t_x = r_p^{-1}(-x)$ or $x_t = -r_p(t)$. Thus, the derivative r_p' is the growth rate. For the embryo to elongate a certain distance dx, more time is needed for a smaller r_p'. Meanwhile, since every single somite is produced from one cycle of the segmentation clock, in species with a "quicker" segmentation clock, or where the growth rate is slow compared to the segmentation clock rate, there will be an increased number of smaller-sized somites [14].

The above profile of γ can only generate such a parallel spatiotemporal pattern so that the position curve of the new somites (determination front) is a parallel shift of the position curve of the posterior end, with an offset of a specific time. However, many biological data (e.g., Fig. 7 in the Supporting Information of [27]) show that it is possible for the two position curves to become closer during embryo growth, especially in the late stage of somitogenesis. This is why we conclude with another reasonable scenario considering the inhibition on γ. As shown in Fig. 3(c) and Eq. (8), the curve of the determination front where the waves stop is not fully dependent on the growth rate of the embryo.

V. CONCLUSION

In this paper, we proposed a simple reaction-diffusion model with features of (1) discreteness and (2) absence of inhibitor coupling. Those features are biologically important and provide a different scenario of spatially periodic pattern formation from Turing model. Especially the effect of "wave propagation failure" of discreteness makes it possible to produce a robust stationary pattern in bistable excitable medium.

The biological relevance of our model to somitogenesis were discussed in detail. A well agreement to experimental observation was shown. Moreover, we inferred some important physical aspects that are independent of the details of biomolecular reactions. We made an order-of-magnitude conclusion of two valid length scales ($\sqrt{D\tau_2}$ and $\sqrt{D\tau_1}$) based on the interaction among neighboring cells. The comparison between these two theoretical estimation and experimental measurement proved the importance of discreteness and gave a strong support to the rationality of the model.

ACKNOWLEDGMENT

We thank Dr. Aitor González (Institute for Virus Research, Kyoto University, Kyoto, Japan) for comments that helped to improve the article.

[1] A. M. Turing, Philos. Trans. R. Soc. London, Ser. B **237**, 37 (1952).
[2] A. Gierer and H. Meinhardt, Kybernetik **12**, 30 (1972).
[3] J. D. Murray, *Mathematical Biology I: An Introduction*, 3rd ed. (Springer-Verlag, Berlin, 2002), Vol. 1.
[4] S. Sick, S. Reinker, J. Timmer, and T. Schlake, Science **314**, 1447 (2006).
[5] S. Kondo and R. Asai, Nature (London) **376**, 765 (1995).
[6] J. J. Tyson, K. A. Alexander, V. S. Manoranjan, and J. D. Murray, Physica D **34**, 193 (1989).
[7] H. Levine and W. Reynolds, Phys. Rev. Lett. **66**, 2400 (1991).
[8] A. Tero, R. Kobayashi, and T. Nakagaki, Physica D **205**, 125 (2005).
[9] G. Bub and A. Shrier, Chaos **12**, 747 (2002).
[10] Considering the general cell diameter $R \sim 10$ μm, and a diffusion constant in the order of $D \sim 10^{-6}$ cm$^2/s$, we can estimate the time length, in which substances diffuse cross the cell, as $\Delta t \sim R^2/D = 1$ s. On the other hand, time scale of cell dynamics such as oscillation is in the order of hours.
[11] J. P. Keener, SIAM J. Appl. Math. **47**, 556 (1987).
[12] Y. Saga and H. Takeda, Nat. Rev. Genet. **2**, 835 (2001).
[13] Y. Bessho and R. Kageyama, Curr. Opin. Genet. Dev. **13**, 379

(2003).
[14] C. Gomez, E. M. Ozbudak, J. Wunderlich, D. Baumann, J. Lewis, and O. Pourquié, Nature (London) **454**, 335 (2008).
[15] M. Pechmann, A. P. McGregor, E. E. Schwager, N. M. Feitosa, and W. G. M. Damen, Proc. Natl. Acad. Sci. U.S.A. **106**, 1468 (2009).
[16] Y. Bessho, H. Hirata, Y. Masamizu, and R. Kageyama, Genes Dev. **17**, 1451 (2003).
[17] P. C. G. Rida, N. L. Minh, and Y.-J. Jiang, Dev. Biol. **265**, 2 (2004).
[18] O. Cinquin, Mech. Dev. **124**, 501 (2007).
[19] O. Pourquié, Science **301**, 328 (2003).
[20] B. C. Goodwin, Adv. Enzyme Regul. **3**, 425 (1965).
[21] S. Hastings, J. Tyson, and D. Webster, J. Differ. Equ. **25**, 39 (1977).
[22] J. Lewis, Curr. Biol. **13**, 1398 (2003).
[23] T. Y.-C. Tsai, Y. S. Choi, W. Ma, J. R. Pomerening, C. Tang, and J. E. Ferrell, Science **321**, 126 (2008).
[24] H. Hirata, Y. Bessho, H. Kokubu, Y. Masamizu, S. Yamada, J. Lewis, and R. Kageyama, Nat. Genet. **36**, 750 (2004).
[25] J. Cooke and E. E. Zeeman, J. Theor. Biol. **58**, 455 (1976).
[26] I. Palmeirim, D. Henrique, D. Ish-Horowicz, and O. Pourquié, Cell **91**, 639 (1997).
[27] Y. Masamizu, T. Ohtsuka, Y. Takashima, H. Nagahara, Y. Takenaka, K. Yoshikawa, H. Okamura, and R. Kageyama, Proc. Natl. Acad. Sci. U.S.A. **103**, 1313 (2006).
[28] R. E. Baker, S. Schnell, and P. K. Maini, J. Math. Biol. **52**, 458 (2006).
[29] R. E. Baker, S. Schnell, and P. K. Maini, Dev. Biol. **293**, 116 (2006).
[30] K. I. Mazzitello, C. M. Arizmendi, and H. G. E. Hentschel, Phys. Rev. E **78**, 021906 (2008).
[31] N. Armstrong, K. Painter, and J. Sherratt, Bull. Math. Biol. **71**, 1 (2008).
[32] M. Santillán and M. C. Mackey, PLoS ONE **3**, e1561 (2008).
[33] K. Uriu, Y. Morishita, and Y. Iwasa, J. Theor. Biol. **257**, 385 (2009).
[34] H. Meinhardt, *Somites in Developing Embryos* (Plenum, New York, 1986), pp. 179–189.
[35] M. Kerszberg and L. Wolpert, J. Theor. Biol. **205**, 505 (2000).
[36] J. Jaeger and B. C. Goodwin, J. Theor. Biol. **213**, 171 (2001).
[37] J. Hu, L. Doan, D. Currle, M. Paff, J. Rheem, R. Schreyer, B. Robert, and E. Monuki, Proc. Natl. Acad. Sci. U.S.A. **105**, 3398 (2008).
[38] D. Yu and S. Small, Curr. Biol. **18**, 868 (2008).
[39] M. Ibañes and J. C. I. Belmonte, Mol. Syst. Biol. **4**, 176 (2008).
[40] J. Dubrulle, M. J. McGrew, and O. Pourquié, Cell **106**, 219 (2001).
[41] A. Aulehla and B. G. Herrmann, Genes Dev. **18**, 2060 (2004).
[42] R. D. del Corral, I. Olivera-Martinez, A. Goriely, E. Gale, M. Maden, and K. Storey, Neuron **40**, 65 (2003).
[43] P. P. Tam, J. Embryol. Exp. Morph. (Suppl.) **65**, 103 (1981).
[44] J. J. Tyson and J. P. Keener, Physica D **32**, 327 (1988).
[45] N. G. V. Kampen, *Stochastic Processes in Physics and Chemistry* (North-Holland, Amsterdam, 1992).
[46] Y. Togashi and K. Kaneko, Phys. Rev. E **70**, 020901(R) (2004).
[47] H. Hirata, S. Yoshiura, T. Ohtsuka, Y. Bessho, T. Harada, K. Yoshikawa, and R. Kageyama, Science **298**, 840 (2002).
[48] J. Comte, S. Morfu, and P. Marquié, Phys. Rev. E **64**, 027102 (2001).